Budapest University of technology and Economics
Faculty of Mechanical Engineering
Department of Hydrodynamic Systems

Spherical bubble dynamics and cavitating vortex shedding

Booklet of the PhD Dissertation

Written by: Ferenc Hegedűs
M.Sc. in Mechanical Engineering

Supervisor: Dr. László Kullmann
associate professor

June 29, 2012, Budapest

Chapter 1

Dynamics of spherical bubbles

1.1 Introduction

In common engineering applications such as turbomachinery and hydraulic systems cavitation occurs as sheet cavitation or bubble swarm resulting in a limited applicability of the research achievements on a single spherical bubble. For a long time the numerical results obtained from single bubble simulations were used only to understand the mechanism of cavitation damaging by estimating the maximum temperature and pressure during the bubble motion. Recently, however, there are various special applications in which the spherical assumption for a single bubble is valid.

Most of the results in this thesis intend to aid the rapidly developing ultrasonic technology. The main aim of these applications is to enhance the mass, heat and momentum transfer between the various phases by making use of the extreme conditions of the collapse of a cavitation bubble. These are the very high pressure and temperature or the induced shock wave. Thus, the cavitation does not need to be avoided. The engineering applications are mainly related to the food industry and material chemistry (sonochemistry). Some of these are discussed in the following.

The extraction of organic compounds can be enhanced by generating cavitation bubbles with high power ultrasound. The collapsing bubbles improve the penetration depth of the solvent into the cellular material and thus improve the mass transfer between the interfaces, see Vinatoru 2001, Knorr 2003, Li et al. 2004

During the collapse of cavitation bubbles shock waves are generated causing very efficient mixing of two immiscible liquids. Canselier et al. 2002 and Freitas et al. 2006 reported the production of fine, highly stable emulsions.

The alteration of the viscosity of many food systems such as tomato puree is also possible with ultrasound since cavitation causes shear stress that decreases the viscosity of thixotropic fluids. With high enough energy the alteration becomes permanent by reducing the molecular weight of the substances. An example for viscosity reduction was

published by Seshadri et al. 2003.

A promising technology in food preservation is the ultrasonic pasteurization. At moderate temperature (50^oC degree of Celsius) the membrane of the bacterial organisms weakens enough to become less resistant to cavitational damaging. With this novel innovation Knorr et al. 2004 could successfully reduce the E. coli in liquid whole egg.

The extreme conditions at the bubble collapse (very high pressure and temperature) are the driving effects of chemical reactions in various organic/inorganic solutions. The research for new polymers attracts great interest recently in polymer industry. A number of studies reported that high intensity ultrasound reduces the molecular weight of a polymer in solution by reducing the chain length via shock waves emitted by bubble collapses, see e.g. Konaganti and Madras 2010. Using two kinds of polymers in a common solvent, the macromolecular fragments with free radicals lead to formation of new copolymers.

As heterogeneous catalysis often required rare and expensive metals, it can be very useful to activating less reactive, but much cheaper metals. Recent investigations revealed that the ultrasonic radiation can increase the catalytic processes by increasing the effective surface area. This phenomenon is also due to the cavitation-induced shock waves. A comparison between conventional and ultrasound-mediated heterogeneous catalysis was performed by Disselkamp et al. 2004.

1.2 Periodic solutions of the Rayleigh–Plesset equation

The rapidly spreading ultrasonic technology motivated me to investigate a spherical bubble under harmonically varying pressure field by applying high amplitude p_A and high angular frequency ω sound field to the liquid domain. I also noted that although the computations were performed with water at specific ambient pressure and temperature employing the simplest and still widely used bubble model, the Rayleigh–Plesset equation, the results are qualitatively the same for other substances and ambient properties due to the structural stability of the bubble oscillation. The bubble interior contains vapour and non-condensable gas. The nonlinear nature of the model results in the existence of various kinds of stable oscillations simultaneously. As the different kinds of oscillations have different properties, it is important to know the evolution of each solution under parameter variations. Therefore, I intend to find the period 1, 2 and 3 solutions (meaning that the period of the solution is 1, 2 and 3 times the period of the excitation) in the parameter space of the relative angular frequency ω_N and pressure amplitude p_A providing parametric maps of the global dynamics for experiments. Figure 1.1 summarizes these regions; blue, brown and green regions correspond to the existence of period 1, 2 and 3 attractors, respectively. In Fig. 1.1 ω_o is the natural angular frequency.

Due to the strong nonlinearity of the system, the different kinds of attractors usually

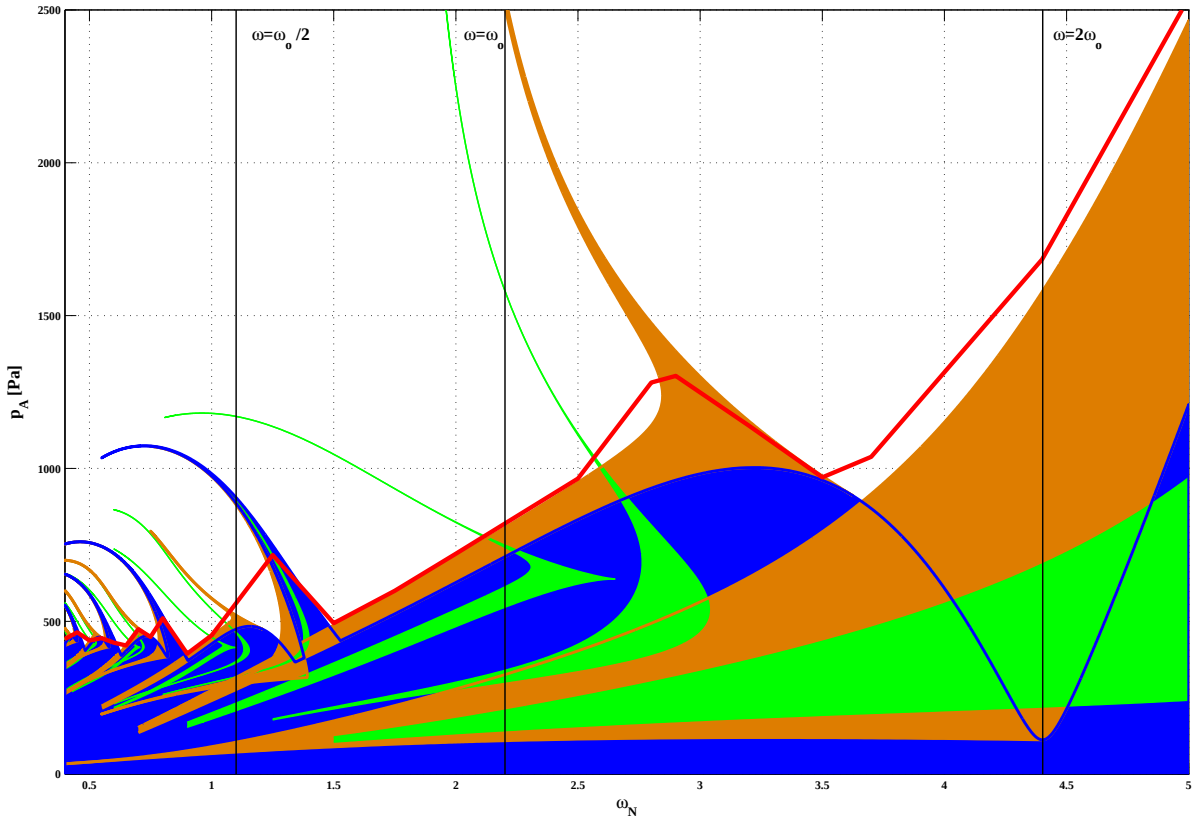

Figure 1.1: Summary of the regions where period 1, 2 and 3 attractors exist in the $p_A - \omega_N$ plane. The blue, brown and green regions correspond to the period 1, 2 and 3 attractors, respectively. The red line depicts a practical stability limit obtained numerically from the IVP computations.

coexist. The examination of the domain of attractions at $\omega = 2\omega_o$ revealed that the chance to find a period 3 solution is very low. Their basin of attraction is no more that 4% of the global basin. This means that only 4 out of 100 bubble may exhibit collapse-like motion.

The global basin could be computed up to the pressure amplitude $p_A = 450\,\mathrm{Pa}$ as enclosed area of the stable manifolds of a saddle-type unstable solution. Above this point the invariant manifolds intersect each other and the boundary of the basin becomes fractal. The inception of the tangency was predicted by Melnikov's method based on the perturbation of a planar homoclinic orbit. Unfortunately, it gave a poor estimation ($p_A = 840\,\mathrm{Pa}$ instead of $p_A = 450\,\mathrm{Pa}$).

Thesis #1:

The presence of the period 1, 2 and 3 attractors in the pressure amplitude-relative frequency ($p_A - \omega_N$) parameter plane of the harmonically excited Rayleigh–Plesset equation was explored assuming isothermal state of change for the gas.

- It was found that the domain in the $p_A - \omega_N$ plane, where stable solutions exist increases linearly with the frequency if $\omega > 2\omega_o$, ω_o being the natural angular frequency.
- At $\omega = 2\omega_o$, the attracting domain of the period 3 attractor is less than 4% of the global domain of attraction.
- The boundary of the global basin of attraction becomes fractal at $p_A = 450\,\mathrm{Pa}$ due to the homoclinic tangency of the invariant manifolds of the saddle type orbit, bifurcating from the unstable equilibrium point of the unexcited system.
- An estimation was given by Melnikov's perturbation method for the critical pressure amplitude of the homoclinic tangency. It was found that, for the parameter values of engineering importance (viscosity and pressure amplitude) it provides results with limited accuracy ($p_A = 840\,\mathrm{Pa}$ as opposed to the exact value of $450\,\mathrm{Pa}$).

The publications related to this thesis are Hegedűs et al. 2012a, Hegedűs and Kullmann 2012c, Hegedűs et al. 2011, 2009c.

1.3 The influence of heat transfer on bubble dynamics

If the bubble contains also vapour then during the bubble motion condensation and evaporation processes take place. The required or excess heat arrives or leaves via heat conduction from or into the liquid domain. In the Rayleigh–Plesset (RP) equation this phenomenon is not modelled, the temperature field in the liquid is assumed to be homogeneous, which is equivalent to an infinitely fast heat transfer rate between the two phases. In order to investigate this effect one has to attach the conservation equation of the energy to the Rayleigh–Plesset equation (RPH model).

From the numerical point of view, my primary goal was to decompose the partial differential equation of the heat transfer into an ordinary differential equation system via some sort of semi-discretization procedure. This treatment has many advantages, it allows an efficient (higher order) and adaptive time marching such as the Runge–Kutta solvers, in addition, the method of nonlinear bifurcation analysis can be applied. One of the fundamental methods is based on the finite difference spatial discretization scheme. Although it requires a large number of equations to achieve high accuracy, it is used

for reference computations due to its superior stability properties. The fact, that the computation of periodic orbits can be very resource demanding inspired me to apply higher order spectral methods (Galerkin and the spectral collocation) in order to reduce the number of the equations (DoF) as much as possible.

From a comprehensive numerical investigation it was found that for moderate spatial resolution (up to 30 DoF) the Galerkin technique with hat functions as a basis provides the most accurate solution, while, for finer resolution, the spectral collocation technique and polynomial-based Galerkin method are superior.

Comparing the simple RP equation and the RPH model, it turned out that the heat transfer process plays a significant role by two mechanisms. First, if the ambient properties (temperature and pressure) are close to the tension curve, since, in this case the concentration of the vapour becomes comparable to the non-condensable gas. Second, there is an explicit dependence on the temperature itself, which is a consequence of the fact that the quantity $\lambda/(\rho_V L)$ in the boundary condition at the interface governing the heat transfer through the bubble wall decreases with the temperature. It falls from 100% to 17% as the ambient temperature is increased from 30^oC to 70^oC, independently of the system pressure.

Thesis #2:

The effect of heat transfer on the bubble motion was studied by extending the Rayleigh–Plesset equation with the equation of energy in the liquid domain. The analysis of various semi-discretization methods applied to the equation of energy revealed that:

- For moderate discretization level (less than 30 degrees of freedom) the Galerkin technique with hat functions as basis provides the most accurate solution.
- If finer spatial resolution is needed, the spectral collocation or polynomial-based Galerkin method has to be employed.

The publications related to this thesis are Hegedűs et al. 2010a, 2009b, 2008.

Thesis #3:

The heat transfer significantly affects the bubble dynamics by two mechanisms:

- First, if the ambient pressure and temperature are close to the tension curve. In this case the partial pressure of the non-condensable gas becomes less significant. The large concentration of vapour enhances the effect of the heat transfer since the vapour concentration determines the rate of the evaporation and condensation processes.

- Second, in the case of high ambient temperature. The coefficient $\lambda/(\rho_V L)$ in the boundary condition at the interface decreases very rapidly with the ambient temperature in the examined parameter region, thereby significantly reducing the bubble wall velocity $\dot{R}$.

The publication related to this thesis is Hegedűs et al. 2010a.

1.4 Measurements on the free oscillations of a single bubble

The consequence of the heat conduction equation extending the Rayleigh–Plesset equation is that at least two additional parameters appear in the model, namely, the thermal diffusivity and the latent heat. They both cannot be eliminated via dimensional analysis. The different number of the parameters may encumber the investigation of the two models together; hence, some sort of method has to be developed to make the comparison precise. The concept is based on the fact that all material properties depend in general on two state variables for pure substances. Regarding the ambient pressure P_∞ and temperature T_∞ as the main variables, the number of the parameters can be significantly reduced. Moreover, as expected, all the remaining parameters are identical in every model, namely, the above-mentioned pressure, temperature and the equilibrium bubble size describing the amount of the non-condensable gas.

Consequently, beside the measurement of time histories of the bubble radius, we intend to develop a measurement process for the validation of different bubble models keeping in mind that the two main parameters are the temperature T_∞ and the pressure P_∞. For this reason, a suitable device (vacuum chamber) had to be designed in which the ambient properties could be adjusted arbitrarily. The details of the chamber, the temperature regulation and the manufacture process were carried out in the Department of Hydrodynamic Systems of the Budapest University of Technology and Economics.

Using the vacuum chamber, the free oscillation of a single spherical gas bubble in glycerol was examined experimentally at different ambient temperatures ($25\,^\circ\mathrm{C} - 60\,^\circ\mathrm{C}$) and pressures ($250\,\mathrm{mbar} - 1000\,\mathrm{mbar}$). The bubble was generated using a Q-switched 6 ns Nd:YAG laser. The temporal history of the radius was measured by a novel shadowing technique developed at Hochschule Emden/Leer, University of Applied Sciences that is capable of resolving the much different time scales of the oscillations. Applying the novel measurement method, the Rayleigh–Plesset and the Keller–Miksis equations were validated in the T_∞ - P_∞ parameter plane. The bubble equilibrium radius R_E was in the order of tenth of millimetres.

Figure 1.2. shows a series of results in which the black curve is the measurement, while the red and blue curves are the results from the Keller–Miksis and the Rayleigh–Plesset equations, respectively. From the results it is clearly seen that the Keller–Miksis

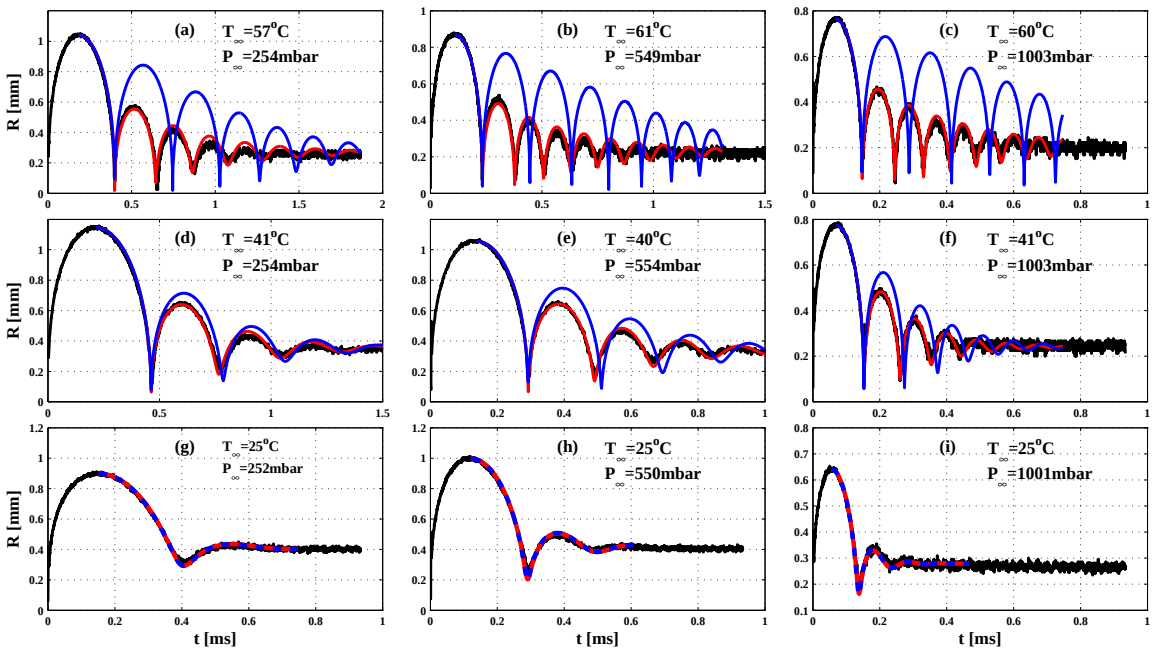

Figure 1.2: Comparison of the measurement and the results obtained from the models at different temperature and pressure values. The black, red and blue curves are the results of the measurement, Keller–Miksis and Rayleigh–Plesset equation, respectively. In subfigures (a) to (c) the black and the red lines are nearly congruent.

equation agrees well with the experimental data in every case. On the other hand, the Rayleigh–Plesset equation can provide extremely poor results.

Thesis #4:

A method was developed which is capable of comparing different bubble models which is based on the fact that the material properties of a pure substance depend only on the ambient temperature and the pressure.

In order to produce arbitrary temperature and pressure values a vacuum chamber was designed which was manufactured at the Department of Hydrodynamic Systems of the Budapest University of Technology and Economics.

Applying the novel bubble radius measurement technique developed in Hochschule Emden/Leer, University of Applied Sciences together with the vacuum chamber the Rayleigh–Plesset and the Keller–Miksis equations was validated.

The publications related to this thesis are Hegedűs et al. 2010a and Koch et al. 2012b.

Chapter 2

Cavitating Vortex Shedding

2.1 Measurements on the cavitation channel

In this chapter the experiments in the large cavitation channel of the Department of Hydrodynamic Systems of the Budapest University of Technology and Economics will be presented. Two models (square cylinders) with side lengths 50 mm and 25 mm were placed in the 200 mm high and 50 mm wide test section, thus the blockage ratio was 25% and 12.5%, respectively. The range of Reynolds number was between $2.5 \cdot 10^4$ and $4.7 \cdot 10^5$

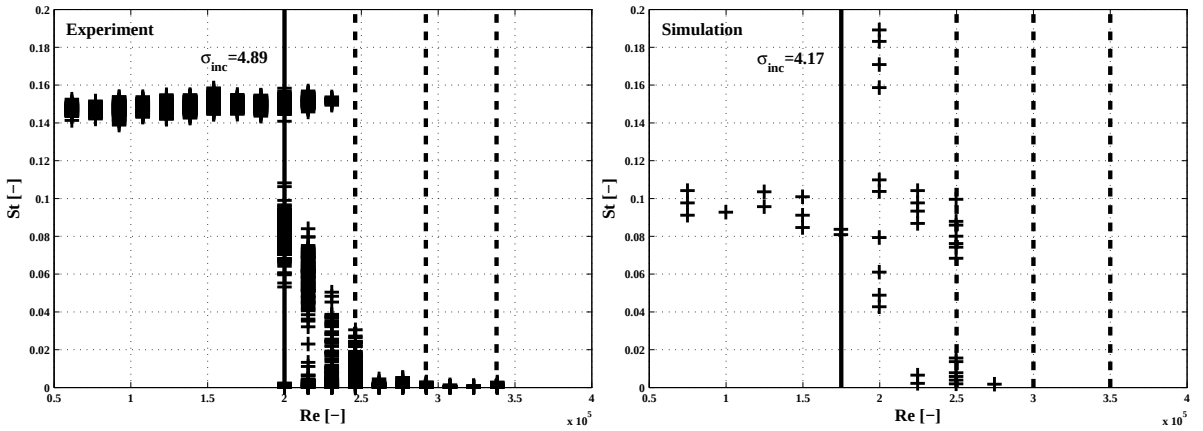

Figure 2.1: The comparison of the Reynolds number - Strouhal number relationship of the experiment ($H = 25\,\text{mm}$) and the numerical simulation.

which is a natural extension of the values found in the literature.

Although, various models with different shapes can be placed in the test section, I decided to use square cylinders in order to compare the results with CFD simulations easier (simple meshing, fixed separation point). My experimental results were compared with the numerical simulations of Roland Rákos, who used the ANYSY CFX v10.0 commercial

software. The model height was 20 mm and the blockage ratio was 5%.

The main outcome of this investigation is the relationship between the Reynolds and the Strouhal number. Our experimental results show good agreement with the literature from which it turned out, that the dominant Strouhal number seems to be stabilized and is independent from the Reynolds number, see Fig. 2.1. After the inception of cavitation the Strouhal number remains constant up to the supercavitational regime. Because the moderate level of cavitation has no influence to the vortex shedding frequency and therefore to the Strouhal number, the vortex flow meters can provide reliable data even if cavitation takes place.

Thesis #5:

The vortex shedding behind square cylinders with different side lengths were investigated experimentally in the cavitation channel of the Department of Hydrodynamics Systems of Budapest University of Technology and Economics.

- The range of the Reynolds number applied in the literature in the experiments was extended from 10^5 up to $4.7 \cdot 10^5$. In the range of Re$< 10^5$ the measurement results (Strouhal numbers) were consistent with the corresponding literature.
- The cavitating flow has no influence on the value of the Strouhal number; it remains constant up to the point where supercavitation is formed.

The publications related to this thesis are Hegedűs et al. 2010b,c, Hegedűs and Kullmann 2009a.

Own publications

Hegedűs, F., Hős, Cs., Kullmann, L., 2012. Stable period 1,2 and 3 structures of the harmonically excited Rayleigh–Plesset equation low ambient pressure. IMA J. Appl. Math., in press, DOI:10.1093/imamat/hxs016. (IF:0.653)

Koch, S., Garen, W., Hegedűs, F., Neu, W., Teubner, U., 2012. Time-resolved measurements of shock-induced cavitation bubbles in liquids. Appl. Phys. B - Lasers O., in press, DOI:10.1007/s00340-012-5070-1. (IF:2.239)

Hegedűs, F., Kullmann, L., 2012. Basins of attraction in a harmonically excited spherical bubble model. Per. Pol. Mech. Eng., accepted.

Hegedűs, F., Hős, Cs., Kullmann, L., 2011. An analysis of the periodic solutions of an acoustically excited cavitation bubble. In: 19th International Conference in Mechanical Engineering (OGÉT 2011), Sumuleu-Ciuc, Romania, 160–163.

Hegedűs, F., Hős, Cs., Kullmann, L., 2010. Influence of heat transfer on the dynamic response of a spherical gas/vapour bubble. Int. J. Heat Fluid Fl., 31(6), 1040–1049. (IF:1.802)

Hegedűs, F., Hős, Cs., Pandula, Z., Kullmann, L., 2010. Measurement on the cavitating vortex shedding behind rectangular obstacles. In: 25th IAHR Symposium on Hydraulic Machinery ans Systems, Timisoara, Romania; IOP Conf. Series: Earth and Environmental Science 12(1), Paper: 012066.

Hegedűs, F., Mészáros, B., Kullmann, L., 2010. Measurement on cavitating vortex shedding behind a square shaped obstacle. In: Proceedings of the Seventh Conference on Mechanical Engineering (Gépészet 2010), Budapest, Hungary, Paper: 122.

Hegedűs, F., Roland, R., Kullmann, L., 2009. Experimental and numerical study on cavitating vortex shedding behind a square cylinder. Per. Pol. Mech. Eng., 53(2), 55–60.

Hegedűs, F., Hős, Cs., Kullmann, L., 2009. Influence of heat transfer on the dynamic response of a spherical gas/vapour bubble. In: Conference on Modelling Fluid Flow (CMFF'09), Budapest, Hungary, 173-180.

Hegedűs, F., Hős, Cs., Kullmann, L., 2009. Detection of chaotic motions of a harmonically excited cavitation bubble with gas content. In: 17th International Conference in Mechanical Engineering (OGÉT 2009), Gheorgheni, Romania, 156–160.

Hegedűs, F., Kullmann, L., 2008. Rayleigh–Plesset equation stability analysis. In: Proceedings of the Sixth Conference on Mechanical Engineering (Gépészet 2008), Budapest, Hungary, Paper: G-2008-E-02.

Hegedűs, F., Koch, S., Garen, W., Pandula, Z., Paál, Gy., Kullmann, L., Teubner, U., 2012. The effect of high viscosity on compressible and incompressible Rayleigh–Plesset-type bubble models. Int. J. Heat Fluid Fl., need major revision. (IF:1.802)

References

Canselier, J.P., Delmas, H., Wilhelm, A.M., Abismail, B., 2002. Ultrasound emulsification - An overview. J. Disper. Sci. Technol., 23(1-3), 333–349.

Disselkamp, R.S., Judd, K.M., Hart, T.R., Peden, C.H.F., Posakony, G.J., Bond, L.J., 2004. A comparison between conventional and ultrasound-mediated heterogeneous catalysis: hydrogenation of 3-buten-1-ol aqueous solutions. J. Catal., 221(2), 347–353.

Freitas, S., Hielscher, G., Merkle, H.P., Gander, B., 2006. Continuous contact- and contamination free ultrasonic emulsification - A useful tool for pharmaceutical development and production. Ultrason. Sonochem. 13(1), 76–85.

Knorr, D., 2003, Impact of non-thermal processing on plant metabolites. J. Food Eng. 56(2-3), 131–134.

Knorr, D., Zenker, M., Heinz, V., Lee, D-U., 2004, Applications and potential of ultrasonics in food processing. Trends Food Sci. Tech. 15(5), 261–266.

Konaganti, V.K., Madras, G., 2010. Ultrasonic degradation of poly(methyl methacrylate-co-alkyl acrylate) copolymers. Ultrason. Sonochem. 17(2), 403–408.

Li, H., Pordesimo, L., Weiss, J., 2004. High intensity ultrasound-assisted extraction of oil from soybeans. Food. Res. Int. 37(7), 731–738.

Seshadri, R., Weiss, J., Hulbert, G.J., Mount, J., 2003. Ultrasonic processing influences rheological and optical properties of high methoxyl pectin dispersions. Food Hydrocolloid., 17(2), 191–197.

Vinatoru, M., 2001, An overview of the ultrasonically assisted extraction of bioactive principles from herbs. Ultrason. Sonochem. 8(3), 303–313.